Magazine of Civil Engineering

ISSN
2712-8172

journal homepage: http://engstroy.spbstu.ru/

Research article
UDC 691.43
DOI: 10.34910/MCE.138.3

Phase formation, structure and properties of ceramic materials based on binary mixtures “refractory clay – steel slag”

T.V. Vakalova ✉, **N.P. Sergeev**, **D.T. Tolegenov**, **I.B. Revva**

National Research Tomsk Polytechnic University, Tomsk, Russian Federation

✉ *tvv@tpu.ru*

Keywords: refractory clay, steel slag, sintering, mechanical strength, gehlenite, anorthite, building ceramics

Abstract. The work is devoted to the current problem of creating high-strength ceramic materials using techno-genic waste. This problem is solved by using refractory clay as the main raw material component with the addition of high-iron calcium silicate steel slag in various proportions. The processes of phase formation that occur during heating of steel slag are considered. It has been established that the use of steel slag to produce ceramic materials is possible only if the destructive effect of dicalcium silicate formed in the slag at firing temperatures above 1000 °C is neutralized. This is possible due to the chemical transformation of dicalcium silicate into other calcium-containing minerals that are safe from the point of view of molded sample destruction, such as anorthite, wollastonite, gehlenite, and others that do not have polymorphism. Compositions of ceramic masses have been developed that ensure the production of high-strength anorthite ceramics (with water absorption from 2.8 to 13.4 % and compressive strength of up to 200 MPa) for a wide range of purposes – structural (wall) building ceramics, clinker building ceramics, ceramic proppants, etc.

Citation: Vakalova, T.V., Sergeev N.P., Tolegenov, D.T., Revva, I.B. Phase formation, structure and properties of ceramic materials based on binary mixtures “refractory clay – steel slag”. Magazine of Civil Engineering. 2025. 18(6). Article no. 138703. DOI: 10.34910/MCE.138.3

1. *Introduction*

Among building ceramic materials, clinker ceramics have been gaining popularity in the last decade, which is divided into construction (finishing, facade), road (pavement), and technical ceramics. Ceramics are classified as clinker if the value of its water absorption is no more than 6 %, the compressive strength is not less than 30.0 MPa. However, according to some data [1], the compressive strength of building clinker with a water absorption of 2–2.5 % can exceed 200–250 MPa, and with a water absorption of 2–4 %, as a rule, it is higher than 80–100 MPa. In addition to improved quality characteristics, clinker brick has distinctive aesthetic characteristics – color transitions due to a higher firing temperature [2]. The production of products with such properties largely depends on the quality of the clay raw materials used, which must be low-temperature sintered and, preferably, with a wide sintering range (at least 100 °C), which is typical for refractory and ball clays, the deposits of which are quite scarce, and the reserves limited [3]. Replacing at least part of such in short supply clay raw materials in ceramic masses with other, preferably more abundant and cheaper natural or man-made raw materials, would allow for significant savings in high-quality raw materials, which, together with the use of waste, would reduce production costs and improve the environment [4]. Thus, in the context of decreasing reserves of explored natural raw materials, as well as increasing anthropogenic load on the environment, the problem of expanding the areas and volumes of use of industrial waste from the mining, metallurgical, fuel, and energy complexes is of particular importance.

Among man-made waste, a special place is occupied by sludge and slag from metallurgical production. Steel slag is a by-product of processing iron into steel in a converter furnace, or melting scrap to produce steel in an electric arc furnace [5, 6]. Steel slag dumps occupy large areas of land and lead to many serious environmental problems. In this regard, the search for a new, effective way to increase the volume of steel slag recycling is of serious concern. The chemical composition and cooling conditions of molten steel slag have a great influence on its physical and chemical properties in the solidified state. The main chemical compositions of steel slag include CaO, SiO_2, Al_2O_3, Fe_2O_3, MgO, and FeO [7–9]. The common minerals in steel slag are olivine, merwinite, dicalcium silicate (C_2S), tricalcium silicate (C_3S), tetracalcium aluminoferrite (C_4AF), dicalcium ferrite (C_2F), RO phase (CaO–FeO–MnO–MgO solid solution), and free CaO [6, 10, 11]. It is well known that belite C_2S and alite C_3S have binding properties, therefore, steel slag is widely used as an additive to cement and concrete [12–16]. In addition, steel slag is recommended for the production of glass ceramics [17–20], special-purpose ceramics [21–23], and especially for the production of building ceramics [24–26]. The involvement of waste in silicate technologies necessitates the search for new scientific approaches to the selection of raw materials, the development of criteria for assessing the possibility of using such raw materials to obtain high-quality building materials. Solving these problems requires theoretical and exploratory research to find ways and methods for obtaining ceramic and composite structures that ensure the achievement of high mechanical characteristics and other performance properties. The purpose of this work is to study the processes of formation of the phase composition, structure, and physical and mechanical properties of ceramics based on refractory (kaolinite) clay using steel slag in various proportions.

To achieve this objective, it is necessary to solve the following tasks:

- to establish the chemical composition, mineralogical (phase) composition, structural features of the initial steel slag;
- to study structural and phase changes during heating of steel slag;
- to carry out theoretical and exploratory research on the development of compositions and technological parameters for the obtaining of high-strength ceramic materials based on composition of refractory clay and steel slag.

2. Methods

2.1. Characteristics of Initial Raw Materials Used

Refractory clay from the Latnenskoye deposit was used as a clay raw material. According to the chemical composition, it belongs to the main clayey raw material with an average content of coloring oxides (>1.5 % Fe_2O_3 and >1.5 % TiO_2) in the calcined state (Table 1), according to the mineralogical composition – kaolinite-hydromica clay with an admixture of quartz in the coarse part (Fig. 1), in terms of sinterability – high-temperature sintering clay with a sintering temperature above 1200 °C (Fig. 2).

Table 1. Chemical composition of the investigated raw materials.

Raw materials	**Content of oxides, wt. %**									
	SiO_2	**Al_2O_3**	**Fe_2O_3**	**Fe_2O_3**	**MnO**	**CaO**	**MgO**	**K_2O**	**Na_2O**	**LOI**
refractory clay										
Absolutely dry state	49.87	30.55	1.70	1.46	–	1.29	0.67	0.38	0.17	13.91
Calcined state*	57.95	35.50	1.98	1.68	–	1.48	0.77	0.44	0.20	–
steel slag										
Absolutely dry state	7.62	7.80	0.68	21.45	4.72	35.33	8.07	0.09	0.51	3.46
Calcined state*	8.28	8.08	0.70	22.22	4.89	36.60	8.36	0.09	0.52	–

* – after calcination at 950 °C

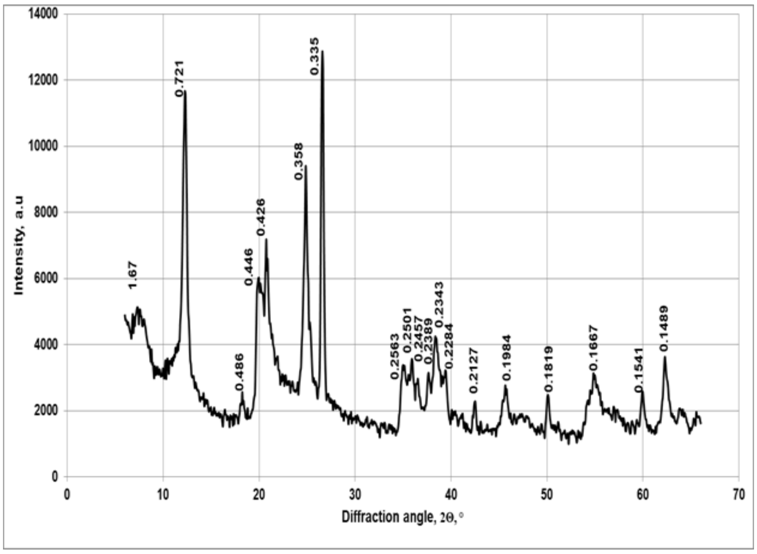

Figure 1. X-ray diffraction pattern of refractory clay used.

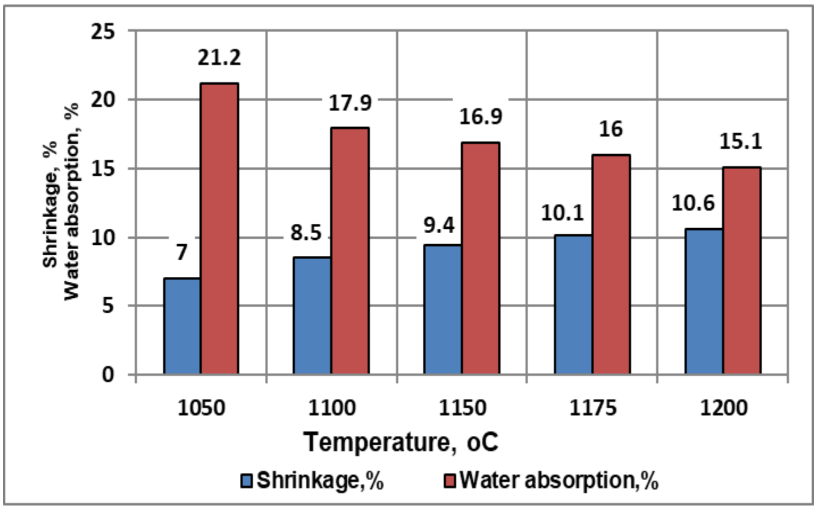

Figure 2. Histogram of changes in the physical and mechanical properties of semi-dry pressing samples from studied clay, fired at 1050–1200 °C.

Steel slag, a waste product from steel production, was tested as a technogenic raw material at the KSP Steel, Republic of Kazakhstan. According to the chemical composition (Table 1), the slag under study is represented mainly by oxides of calcium (35.33 %), iron (21.45 %), silicon (17.62 %), and aluminum (7.80 %), the sum of which is more than 80 %.

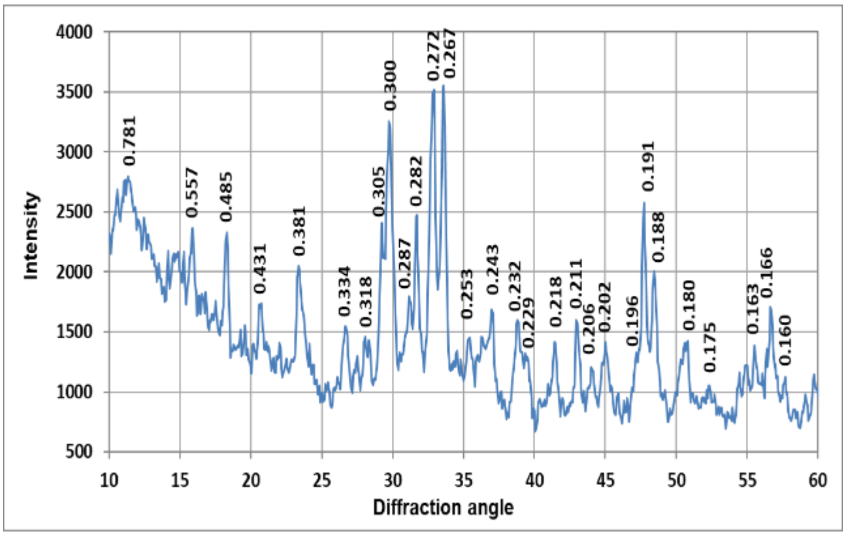

Figure 3. X-ray diffraction pattern of the original steel slag.

A comparative analysis of the chemical composition (Table 1) and X-ray analysis data (Fig. 3) indicates that the calcium component in steel slag is represented by hydrated calcium oxide – portlandite $Ca(OH)_2$, as evidenced by reflections with d/n – 0.492, 0.316, 0.263, 0.193, 0.179 nm, as well as silicates and hydrated calcium silicates – okermanite $2CaO•MgO•2SiO_2$ (0.429, 0.379, 0.306, 0.287, 0.243, 0.232, etc.), tobermorite $5CaO•6SiO_2•5H_2O$ (0.56, 0.306, 0.297 0.282 nm, etc.), and dicalcium hydrosilicate $2CaO•SiO_2•H_2O$ (0.429, 0.379, 0.306, 0.282, 0.273, 0.247 nm, etc.). Aluminate, magnesium, and ferrous components are represented by monocalcium aluminate $CaO•Al_2O_3$ (0.56, 0.46, 0.298, 0.254, 0.243 nm), enstatite $MgO•SiO_2$ (0.316, 0.288, 0.252, 0.245, 0.205 nm), and monocalcium ferrite $CaO•Fe_2O_3$ (0.282, 0.273, 0.268, 0.254, 0.210, 0.181 nm).

2.2. Procedures and Methods

All analyzed clay-slag compositions were grouped into two types: the first group of compositions were mixtures, in which clay was the base, and steel slag was an additive in an amount from 10 to 50 %, the second group of compositions were mixtures, in which the base was steel slag, and clay was added in an amount of 10 to 40 %.

Clay dried to an air-dry state was crushed to a size of less than 0.5 mm, steel slag – to a size of less than 0.063 mm. Prepared clay and steel slag were dosed in a ratio from 90:10 to 10:90 with an interval of 10 %.

The study of the behavior of upon heating refractory clay and steel slag as well as samples from their mixtures was carried out on semi-dry pressing samples in the form of tablets with a diameter of 20 mm and cylinders 20×20 mm. The required degree of compaction of the press powder and the pressure required for this were selected empirically. The optimum pressing pressure was 20 MPa (based on the maximum bulk density of the compacts). The samples were dried to an air-dry state, after which clay samples were fired in the range of 1050–1200 °C, steel slag samples – in the range of 950–1300 °C, and their mixtures – in the range of 1050–1200 °C with an interval of 50 °C and time-exposure at the final temperature for 2 h. The calcined samples were cooled together with a furnace in a free mode.

2.3. Experimental Method

The physicochemical and processing properties of the initial refractory clay and steel slag upon heating, the studied mixtures of refractory clay with steel slag and finished products were investigated using physical and chemical methods. These methods include traditional chemical and elemental analyses by an Oxford XSupreme 8000 X-ray fluorescence analyzer. The phase compositions of the specimens were analyzed via an X-ray diffractometer (Shimadzu XRD-7000S) with $CuK\alpha$ radiation ($\lambda K\alpha$ = 0.154186 nm) at 40 kV and 25 mA. The specimens were tested in the angle range of 10–60° (2θ). Moreover, the crystalline phases were identified on the basis of the experimental patterns using the Powder Diffraction File Database of the International Center for Diffraction Data. The microstructures were observed using a scanning electron microscope (Hitachi S-570 and JEOL JSM-840).

Air and fire shrinkage was determined on the tablet samples. Drying shrinkage of samples were measured by controlling of sample length, width, and height before and after drying process. The measurements of water absorption were performed via the Archimedes method. The compressive strength of the fired samples was measured by using cylindrical samples. The reported compressive strength (MPa) is the average of five measurements.

3. Results and Discussion

3.1. Characteristic of Phase Changes during Heating of the Steel Slag Used

The use of steel slag as raw materials for the production of ceramics makes it necessary to study their behavior when heated.

It was revealed that semi-dry pressing samples from steel slag, fired to 1000 °C, are characterized by high porosity, low strength but still retain their integrity. When heated to 1100 °C, the samples are covered with a network of cracks, and, starting from 1150 °C, they completely crumble after cooling into a fine powder (Fig. 4).

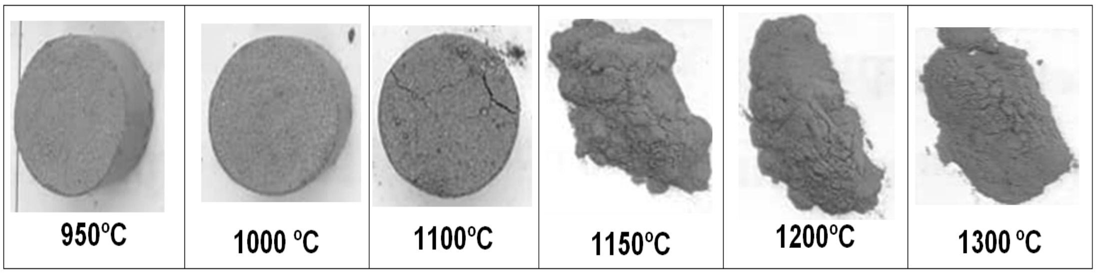

Figure 4. Appearance of molded samples from steel slag, fired at temperatures of 950–1300 °C.

To explain this behavior of the slag when heated, a study was carried out of the phase changes that occur when the slag is heated.

The nature of the ongoing physicochemical processes was considered in two temperature ranges – with low-temperature heating (from 650 to 1000 °C), at which the integrity of the fired samples was maintained (Fig. 5A), and high-temperature heating (from 1100 to 1300 °C), at which the samples completely crumbled (Fig. 5B).

A comparative analysis of X-ray diffraction patterns corresponding to low-temperature heating (Fig. 5A) indicates that heat treatment of metallurgical slag at temperatures up to 1000 °C is accompanied by the following physical and chemical processes leading to a change in the diffraction pattern:

1. Complete dehydration of portlandite, which is manifested in the disappearance in the diffraction pattern of the main reflections of portlandite $Ca(OH)_2$ with interplanar distances d/n – 0.492, 0.316, 0.193, 0.179 nm.
2. The disappearance of reflections at 0.559, 0.297, 0.280 nm at a temperature of 900 °C and the appearance of reflections at 0.255, 0.247, 0.218 nm is due to the process of decomposition of tobermorite $5CaO \cdot 6SiO_2 \cdot 5H_2O$ with the formation of wollastonite $CaO \cdot SiO_2$ and silica [27]:

$$5CaO \cdot 6SiO_2 \cdot 5H_2O \rightarrow 5\left(CaO \cdot SiO_2\right) + SiO_2 + 5H_2O. \tag{1}$$

3. The appearance of X-ray reflections of dicalcium silicate in form γ-$2CaO \cdot SiO_2$ (0.289, 0.279, 0.261, 0.244 nm, etc.) occurs due to the partial dehydration of dicalcium hydrosilicate:

$$2CaO \cdot SiO_2 \cdot H_2O \rightarrow 2CaO \cdot SiO_2 + H_2O. \tag{2}$$

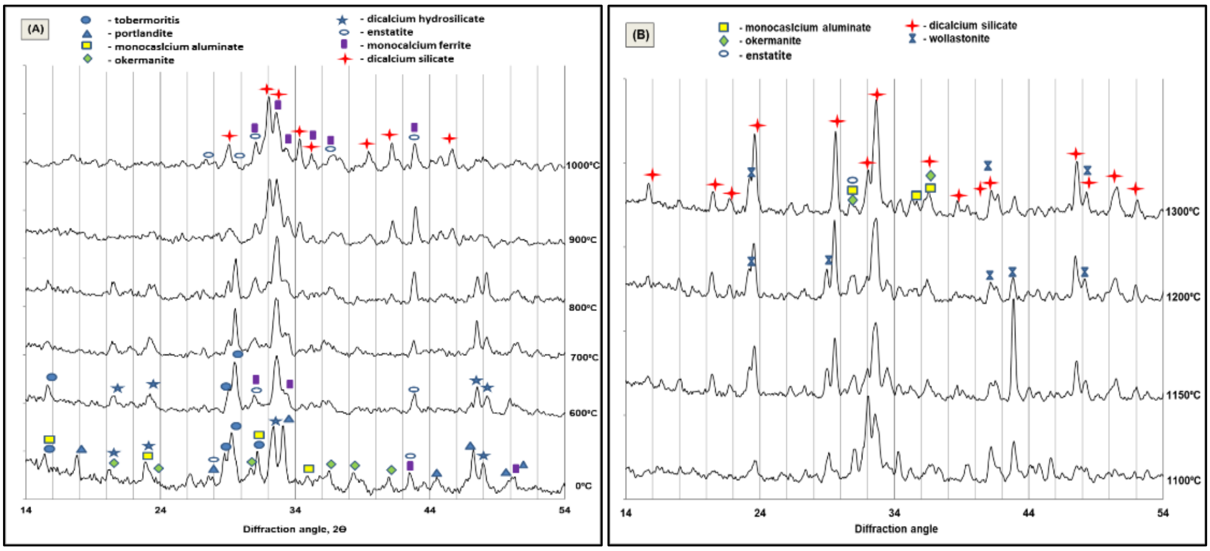

Figure 5. X-ray diffraction patterns of metallurgical slag fired at 600–1000 °C (A) and at 1100–1300 °C (B).

When the firing temperature of pressed samples from the steel slag increases above 1000 °C (Fig. 5B), the diffraction pattern is characterized by:

1. Disappearance of reflections of monocalcium ferrite $CaO \cdot Fe_2O_3$ (0.282, 0.267, 0.254 nm, etc.) at temperature of 1200 °C. This is most likely due to the process of its melting:

$$CaO\cdot Fe_2O_3 \rightarrow \mathit{melt}. \tag{3}$$

2. A sharp increase in the intensity of dicalcium silicate reflections is caused by the completion of the dehydration process of dicalcium hydrosilicate:

$$2CaO\cdot SiO_2\cdot H_2O \rightarrow 2CaO\cdot SiO_2 + H_2O. \tag{4}$$

3. The disappearance of reflections of wollastonite $CaO•SiO_2$ at a temperature of 1200 °C and a sharp increase in reflections of dicalcium silicate γ–$2CaO•SiO_2$ is caused by synthesis of dicalcium silicate due to the reaction:

$$CaO\cdot SiO_2 + CaO \rightarrow 2CaO\cdot SiO_2. \tag{5}$$

Changes in the phase composition of the studied slag during low-temperature (up to 1000 °C) and high-temperature heating (from 1000 to 1300 °C) are given in Table 2.

Table 2. Phase composition of the studied slag before firing and fired up to 1000 °C and above 1000 °C.

Phase	**Formula**	**Presence***		
		in the initial steel slag	**after firing up to 1000 °C**	**after firing above 1000 °C**
portlandite	$Ca(OH)_2$	+	— $Ca(OH)_2 \rightarrow CaO + H_2O$	—
tobermoritis	$5CaO•6SiO_2•5H_2O$	+	— $5CaO•6SiO_2•5H_2O \rightarrow 5(CaO•SiO_2) + SiO_2 + 5H_2O$	—
dicalcium hydrosilicate	$2CaO•SiO_2•H_2O$	+	— $2CaO•SiO_2•H_2O \rightarrow \gamma\text{-}2CaO•SiO_2 + H_2O$	—
okermanite	$2CaO•MgO•2SiO_2$	+	+	+
monocalcium ferrite	$CaO•Fe_2O_3$	+	+	— $CaO•Fe_2O_3 \rightarrow$ melt
monocalcium aluminate	$CaO•Al_2O_3$	+	+	+
enstatite	$MgO•SiO_2$	+	+	+
wollastonite	$CaO•SiO_2$	—	+	+
dicalcium silicate	γ–$2CaO•SiO_2$	—	+ $2CaO•SiO_2•H_2O \rightarrow \gamma\text{-}2CaO•SiO_2 + H_2O$	+ $CaO•SiO_2 + CaO \rightarrow \gamma\text{-}2CaO•SiO_2$

Thus, after firing at 1300 °C, the crystalline phase of the steel slag is represented by a mixture of okermanite $2CaO•MgO•2SiO_2$, monocalcium aluminate $CaO•Al_2O_3$, enstatite $MgO•SiO_2$, wollastonite $CaO•SiO_2$, and dicalcium silicate γ–$2CaO•SiO_2$, the polymorphism of which, when the molded samples are cooled, causes their complete disintegration (Fig. 4) [28]. Therefore, the use of steel slag to produce ceramic materials is possible only if the destructive effect of dicalcium silicate formed in the steel slag at firing temperatures above 1000 °C is neutralized. This is possible due to the chemical transformation of dicalcium silicate into other calcium-containing minerals that are safe from the point of view of molded sample destruction, such as anorthite, wollastonite, gehlenite, and others that do not have polymorphism.

3.2. Theoretical Substantiation of the Choice of the Studied Compositions "Refractory Clay – Steel Slag"

At the first stage, to predict the processes occurring when heating the studied compositions of metallurgical slag with refractory clay, a theoretical analysis of the behavior of the studied compositions in the CaO-Al_2O_3-SiO_2 system was carried out. For this purpose, the chemical compositions of ceramic masses were initially calculated (Table 3).

Table 3. Chemical composition of the investigated mixtures of refractory clay with steel slag.

Mixture code	**Content of oxides, %**								
	SiO_2	**Al_2O_3**	**Fe_2O_3**	**TiO_2**	**MnO**	**CaO**	**MgO**	**K_2O**	**Na_2O**
refractory clay – base, steel slag – additive									
$C_{100}S_0$	57.95	35.50	1.68	1.98	–	1.48	0.77	0.44	0.20
$C_{90}S_{10}$	53.99	32.76	3.74	1.85	0.49	5.00	1.53	0.41	0.23
$C_{80}S_{20}$	50.03	30.02	5.80	1.72	0.98	8.52	2.29	0.37	0.26
$C_{70}S_{30}$	46.06	27.28	7.86	1.60	1.47	12.05	3.05	0.34	0.30
$C_{60}S_{40}$	42.10	24.54	9.92	1.47	1.96	15.57	3.81	0.30	0.33
$C_{50}s_{50}$	38.14	21.80	11.98	1.34	2.45	19.09	4.58	0.27	0.36
steel slag – base, refractory clay – additive									
$S_{100}C_0$	18.33	8.10	22.28	0.70	4.90	36.70	8.38	0.09	0.52
$S_{90}C_{10}$	22.29	10.84	20.22	0.83	4.41	33.18	7.62	0.13	0.49
$S_{80}C_{20}$	26.25	13.58	18.16	0.96	3.92	29.66	6.86	0.16	0.46
$S_{70}C_{30}$	30.22	16.32	16.10	1.08	3.43	26.13	6.10	0.20	0.42
$S_{60}C_{40}$	34.18	19.06	14.04	1.21	2.94	22.61	5.34	0.23	0.39

• here and below, symbol in mixture code corresponds to the type of raw material (C – clay, S – steel slag), number in mixture code – to the content of clay and steel slag, wt.%.

The calculated chemical compositions of the studied compositions indicate that in clay-based compositions with the addition of steel slag, an increase in the steel slag content from 10 to 50 % causes an almost 3–4 times increase in the content CaO (from 5 to 19 %) and Fe_2O_3 (from 3.7 to 12 %) while simultaneously reducing the content of aluminum oxide and silica. In the case of compositions in which steel slag serves as the base and clay as an additive, when the clay content increases from 10 to 40 %, the content of aluminum Al_2O_3 almost doubles (from 10.8 to 21.8 %) and the content of calcium and iron oxides decreases by 2 times (CaO from 33 to 22.6 % and Fe_2O_3 from 20 to 14 %).

Then the multicomponent chemical compositions of the studied mixtures (Table 3) were recalculated to the three-component composition $CaO–Al_2O_3–SiO_2$.

The representative points of the calculated three-component chemical compositions of the studied mixtures were plotted on $CaO–Al_2O_3–SiO_2$ state diagram (Fig. 6)and melting profiles were determined (Fig. 7).

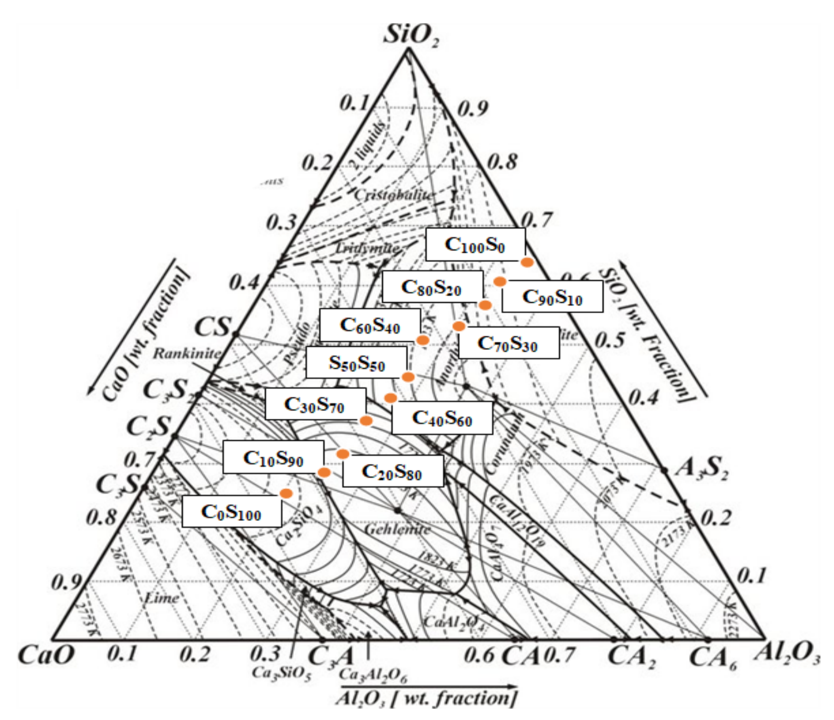

Figure 6. Location of studied compositions of refractory clay with steel slag in $CaO–Al_2O_3–SiO_2$ system.

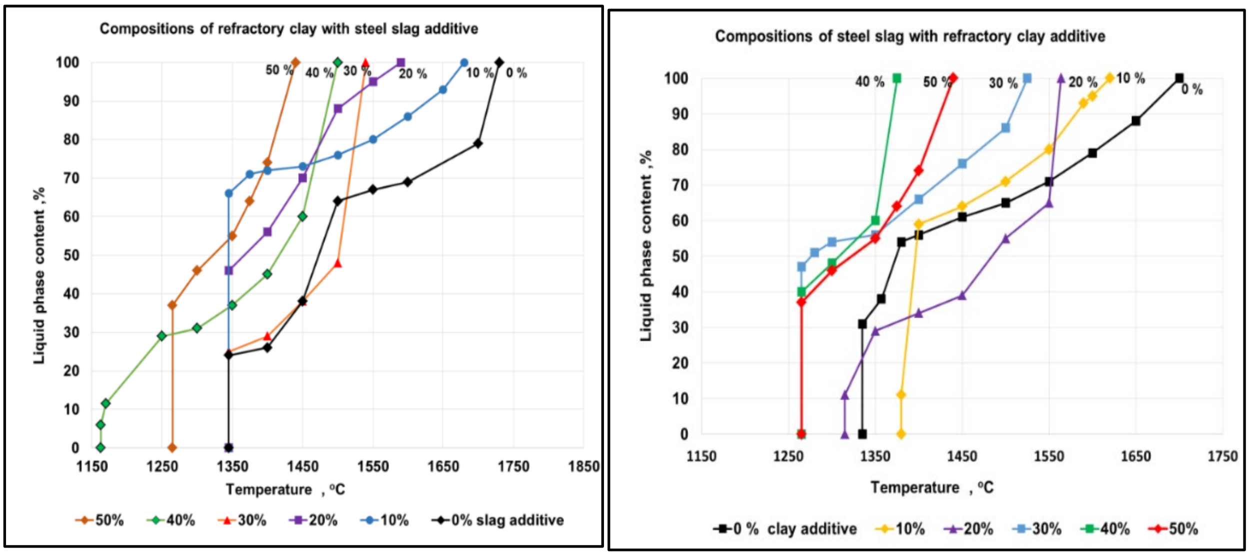

Figure 7. Melting curves of refractory clay with steel slag in CaO–Al_2O_3–SiO_2 system.

Table 4. Characteristics of study mixtures in CaO–Al_2O_3–SiO_2 system.

Mixture code	Addition %	Oxide content, wt. %			Characteristics of the eutectic phase				Complete melting temperature, °C
		CaO	Al_2O_3	SiO_2	Temperature, °C	Eutectic melt content, %	Crystalline phase content, %		
							content, %	dominant phase	
refractory clay – base, steel slag – addition									
$C_{100}S_0$	0	3.03	36.94	60.03	1345	24	76	mullite	1730
$C_{90}S_{10}$	10	8.10	35.68	56.22	1345	66	34		1680
$C_{80}S_{20}$	20	13.22	34.22	52.37	1345	46	54		1590
$C_{70}S_{30}$	30	18.41	33.12	48.47	1345	25	75		1540
$C_{60}S_{40}$	40	23.63	31.82	44.55	1163	6	94	anorthite	1500
$C_{50}S_{50}$	50	29.14	30.42	40.44	1265	37	63		1440
steel slag – base, refractory clay – addition									
$S_{100}C_0$	0	56.22	23.70	20.08	1335	31	69	calcium disilicate	1700
$S_{90}C_{10}$	10	50.64	25.11	24.25	1380	11	89	gehlenite	1620
$S_{80}C_{20}$	20	45.13	26.48	28.39	1315	11	89		1564
$S_{70}C_{30}$	30	39.66	27.84	32.50	1265	47	53		1525
$S_{60}C_{40}$	40	34.27	29.18	36.55	1265	40	60	anorthite	1375

The characteristics of the resulting melts (Table 4) show that, theoretically, the heating behavior of both steel slag and refractory clay in the initial state is very similar. In particular, the temperature, at which the eutectic melt appears, in the slag when heated is 1335 °C in an amount of 31 %, and in clay – 1345 °C in an amount of 24 %. The steel slag will completely melt at 1700 °C, and the refractory clay at 1730 °C. Thus, it has been theoretically revealed that in all mixtures of “refractory clay – steel slag”, in which clay is the main component, additions of steel slag in the amount of 10–50 % (mixtures $C_{90}S_{10}$ – $C_{60}S_{50}$) will activate the sintering process of refractory clay due to sintering the general effect of iron oxide introduced with steel slag (Table 5), with the formation of ceramic materials of predominantly mullite (with 10–30 % slag) and anorthite (40–50 % slag) composition. In “steel slag – refractory clay” compositions, in which steel slag is the basis, the use of refractory clay additives in an amount of 10–40 % (mixtures $S_{90}C_{10}$ – $S_{60}C_{40}$) will reduce not only the temperature of appearance of eutectic melts from 1335 °C (without additives) to 1265 °C (with the addition of clay 30–50 %) but also the temperature of complete melting of these mixtures from 1700 to 1375 °C, transferring them into the category of infusible (with 10–30 % refractory clay) and low-melting (with 40 % refractory clay) ceramic materials gehlenite-anorthite composition.

3.3. *Phase Formation, Structure, and Properties of Ceramics Based on "Refractory Clay – Steel slag" Mixtures*

It has been established that an increase in the firing temperature from 1050 to 1200 °C of semi-dry pressing samples from refractory clay without additives of the studied slag is accompanied by their sintering with a decrease in the value of water absorption from 21 to 15 % (Fig. 8) and providing compressive strength of up to 55 MPa at 1200 °C.

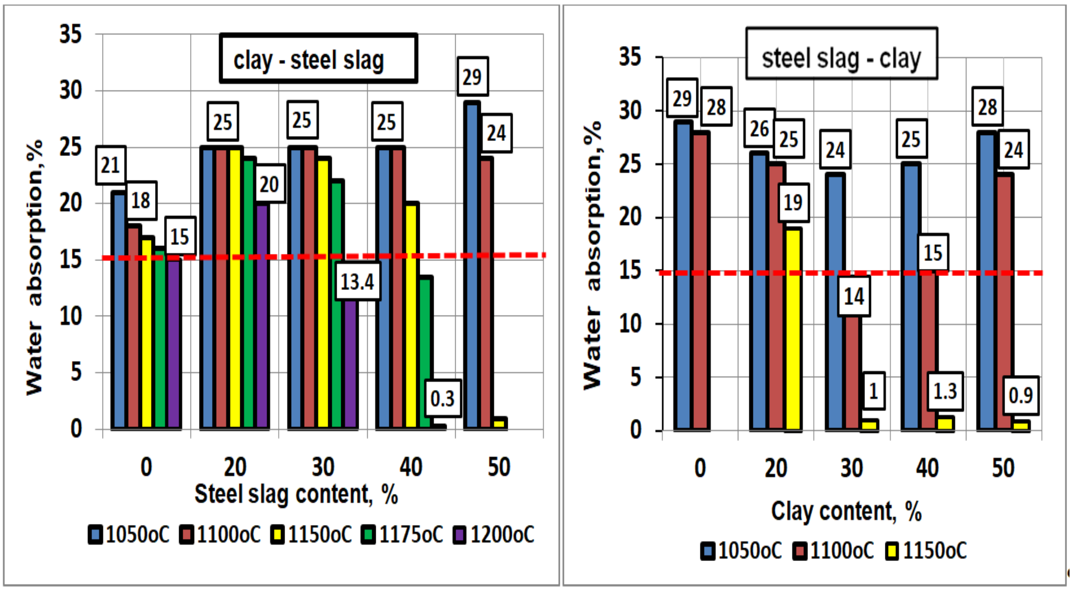

Figure 8. Histogram of changes in water absorption of semi-dry pressing samples from "refractory clay – steel slag" compositions, fired at 1050–1200 °C.

Adding 20 % steel slag to refractory clay leads to a sharp increase in water absorption (up to 25 %) over the entire temperature range. Increasing the content of steel slag additive to 30 % ensures sintering of samples at a temperature of 1200 °C with a density (in terms of water absorption) comparable to the density of clay samples without additive (13.4 and 15 %, respectively) but with almost 2 times greater compressive strength (97 MPa and 55 MPa respectively). A further increase in the amount of steel slag addition from 30 to 40–50 % leads to a sharp activation of the sintering process of the samples, providing a densely sintered state (with water absorption less than 1 %) at 1150 °C (with the addition of 50 % steel slag) – 1200 °C (with the addition of 40 % steel slag). In the case of steel slag compositions with refractory clay additives, as predicted theoretically, clay additives in the entire range of used contents (from 20 to 40 %) and used firing temperatures (1050–1150 °C) not only eliminate the phenomenon of self-disintegration of samples from the original steel slag (for due to synthesis during firing of dicalcium silicate) but also have a sintering-hardening effect, ensuring the formation of densely sintered structures with water absorption of less than 1 % (Fig. 8) and compressive strength from 26 to 56 MPa already at 1150 °C. However, with relatively good strength, all these samples from steel slag compositions with clay additives are deformed at 1150 °C in form of sample center failure from the side of the base in contact with the substrate during firing.

An explanation for these changes should be sought in the study of the physicochemical processes that occur during the firing of these compositions.

The X-ray method made it possible to evaluate changes in the main minerals of the studied refractory clay with the addition of steel slag (Fig. 9) and steel slag with the addition of refractory clay (Fig. 10) in the heating temperature range of 1050–1150 °C.

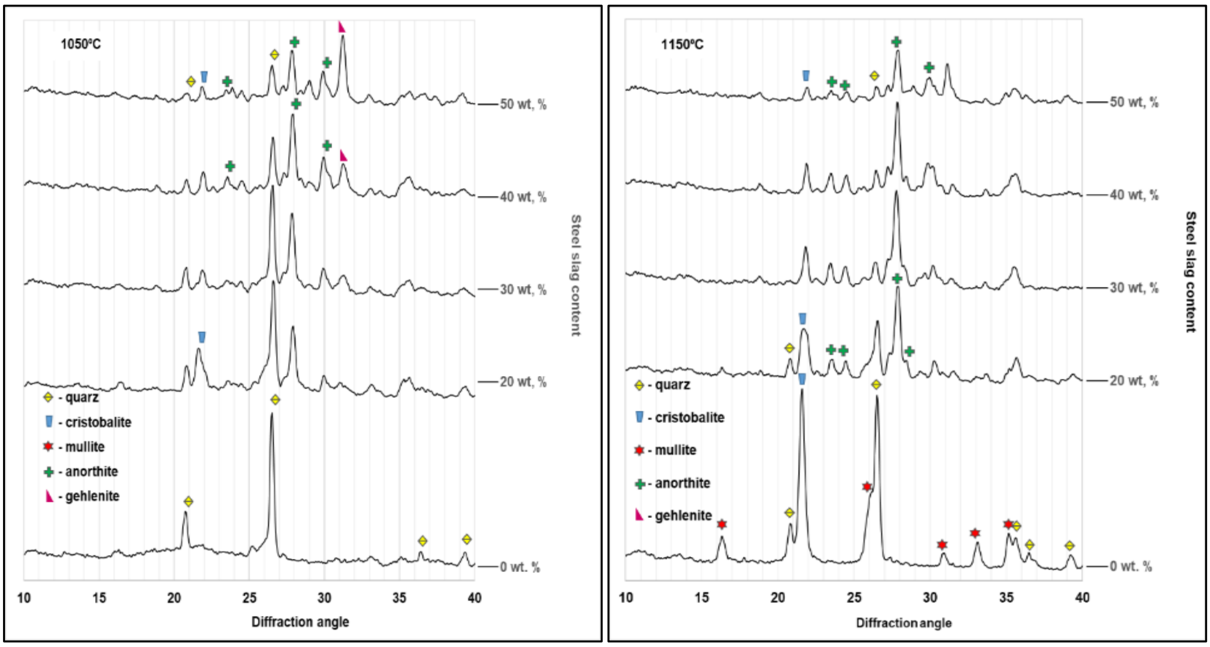

Figure 9. X-ray diffraction patterns of fireclay compositions with steel slag additives at temperatures of 1050 and 1150 °C.

In the case of compositions, in which the base is refractory clay, and steel slag is used as an additive, it was found that even at the minimum of the steel slag contents used (20 wt. %), starting from 1050 °C, in addition to quartz reflections (impurities in clay), cristobalite, and mullite (formed during the thermal dissociation of kaolinite), the presence of anorthite reflections is also recorded.

The preservation of molded samples integrity from all studied mixtures of refractory clay with steel slag additives, as well as the absence of dicalcium silicate reflections in the X-ray diffraction patterns indicates that the formation of anorthite occurs due to the reaction between kaolinite and dicalcium silicate:

$$5\left(\mathrm{Al_2O_3\cdot 2SiO_2\cdot 2H_2O}\right)+\mathrm{2CaO\cdot SiO_2}\rightarrow$$
$$\rightarrow \underset{\text{mullite}}{\mathrm{3Al_2O_3\cdot 2SiO_2}}+2\underset{\text{anorthite}}{\left(\mathrm{CaO\cdot Al_2O_3\cdot 2SiO_2}\right)}+\underset{\text{cristobalite}}{\mathrm{5SiO_2}}+\mathrm{10H_2O}. \qquad (6)$$

An increase in the steel slag content to 30 % at a temperature of 1050 °C is accompanied by a decrease in the intensity of reflections of quartz, cristobalite (due to the presence of clay as a base in the mixture), an increase in the reflections of anorthite, and the appearance of gehlenite reflections:

$$4\left(\mathrm{Al_2O_3\cdot 2SiO_2\cdot 2H_2O}\right)+\mathrm{2CaO\cdot SiO_2}\rightarrow$$
$$\rightarrow \underset{\text{mullite}}{\mathrm{3Al_2O_3\cdot 2SiO_2}}+\underset{\text{gehlenite}}{\mathrm{2CaO\cdot Al_2O_3\cdot 2SiO_2}}+\underset{\text{cristobalite}}{\mathrm{5SiO_2}}+\mathrm{8H_2O}. \qquad (7)$$

With a further increase in the content of the introduced steel slag to the refractory clay to 40–50 %, mullite reflexes disappear, the intensity of gehlenite reflexes increases, which leads to the ratio of the intensity of the anorthite and gehlenite reflections changes in favor of gehlenite:

$$\mathrm{Al_2O_3\cdot 2SiO_2\cdot 2H_2O}+\mathrm{2CaO\cdot SiO_2}\rightarrow \underset{\text{gehlenite}}{\mathrm{2CaO\cdot Al_2O_3\cdot 2SiO_2}}+\underset{\text{cristobalite}}{\mathrm{5SiO_2}}+\mathrm{8H_2O}. \qquad (8)$$

Increasing the firing temperature of samples to 1100 and 1150 °C practically does not change the sequence of phase formation processes in the “refractory clay – steel slag” compositions. And only at a temperature of 1175–1200 °C, when the mixture contains steel slag in an amount of 30–40 % in a mixture with refractory clay, ceramics of an almost anorthite composition is formed.

In the compositions “steel slag – refractory clay” at all applied heating temperatures (from 1050 to 1150 °C) with steel slag (Fig. 10) additive in an amount of 20–30 %, the first synthesized phase is gehlenite formed by reaction (8), and intensity the reflexes of which increase with increasing temperature to 1150 °C.

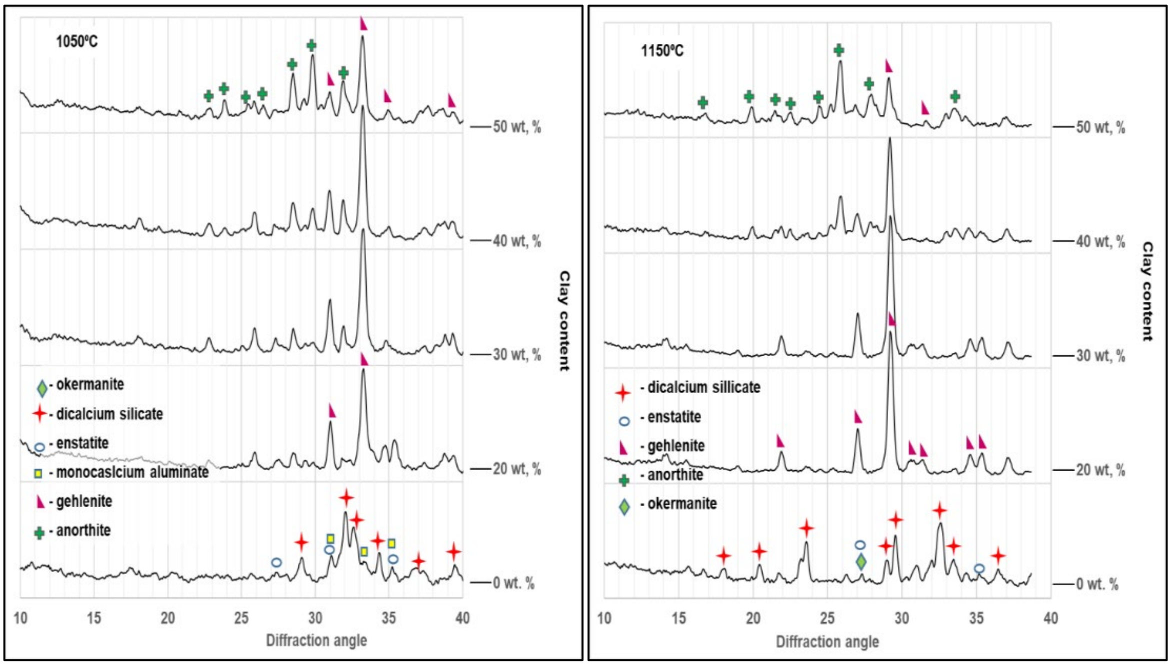

Figure 10. X-ray diffraction patterns of a mixture of steel slag with the refractory clay addition, fired at temperatures of 1050 and 1150 °C.

An increase in the clay additive content from 30 to 40 % causes the synthesis of the second crystalline phase – anorthite throughout the entire range of firing temperatures used. With the addition of 50 % refractory clay, anorthite reflexes increase and the intensity of gehlenite reflexes decreases, especially at 1150 °C. Thus, when adding of refractory clay to the steel slag in an amount of 20–30 % at temperatures of 1050–1150 °C, gehlenite ceramics are formed, when adding of clay in the amount of 40–50 %, ceramics of anorthite-gehlenite composition are formed. The studies carried out make it possible to determine the optimal compositions and technological regimes for obtaining of ceramics based on the studied raw materials (Table 5).

Table 5. Optimum compositions, technological parameters and properties of ceramics based on refractory clay with steel slag.

Composition code	Component composition, %		Firing temperature, °C	Ceramic properties			Type of ceramics
	clay	slag		shrinkage %	water absorption, %	compressive strength, MPa	
clay without steel slag							
$C_{100}S_0$	100	0	1200	10.6	14.2	55.8	mullite-siliceous
clay with steel slag							
$C_{70}S_{30}$	70	30	1200	8.9	13.4	97.2	anorthite
$C_{60}S_{40}$	60	40	1175	8.0	6.3	205.9	anorthite
			1200	13.0	2.8	215.5	

It has been established that the mechanical strength of samples with anorthite crystalline phase (with the addition of 30 % steel slag) is 1.7 times greater than with a mullite crystalline phase (without additive) with almost the same degree of sintering. The strengthening effect of the anorthite crystalline phase on the mechanical properties of building ceramics was previously noted in [29, 30].

Thus, compositions of refractory clay with additions of steel slag from 30 to 40 % at a firing temperature of 1175–1200 °C form ceramic structures with anorthite crystalline phase and compressive strength 1.7–2.8 times higher than the strength of samples from the studied clay without additives (97–215 MPa and 56 MPa, respectively).

Electron microscopy made it possible to evaluate the structure of the fired samples. In particular, electron microscopic images of cleavage of semi-dry pressing samples from the studied clay without the addition of steel slag, fired at 1200 °C (Fig. 11A), as well as samples from a mixture of the studied steel slag with the addition of 40 % refractory clay $S_{60}C_{40}$, fired at 1150 °C (Fig. 11B) show that the samples in both cases at the fracture represent a loosely sintered material, the microstructure of which is represented by individual fine-porous aggregates, separated from each other by deep tortuous pores.

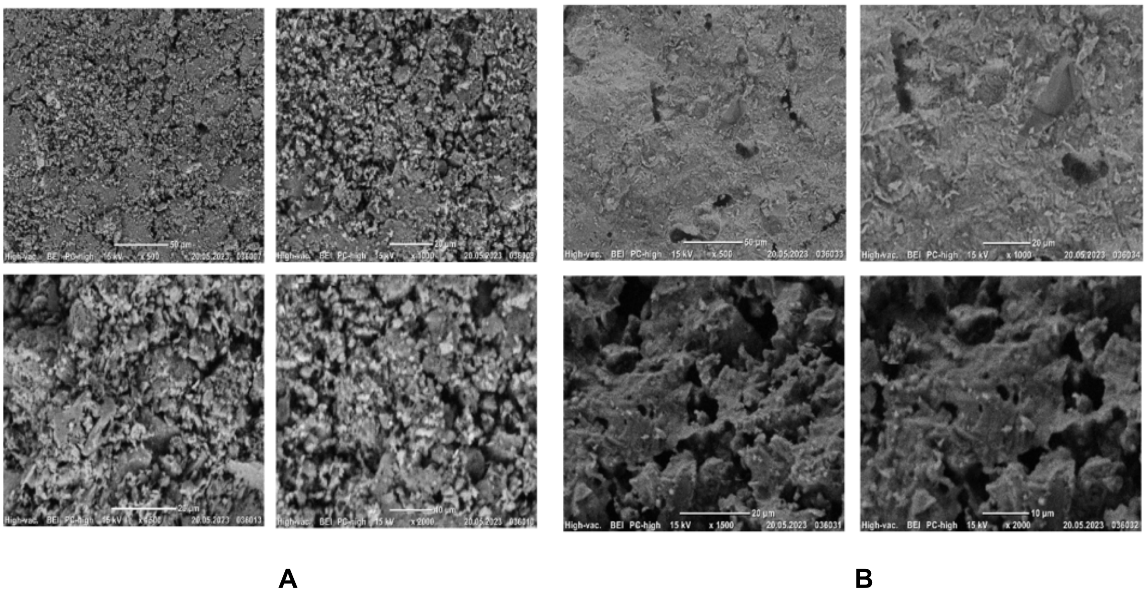
A B

Figure 11. Electron micrographs of cleavage of semi-dry pressed samples made of clay without steel slag (A), fired at 1200 °C, and from a mixture of steel slag with 40 % clay (B), fired at 1150 °C.

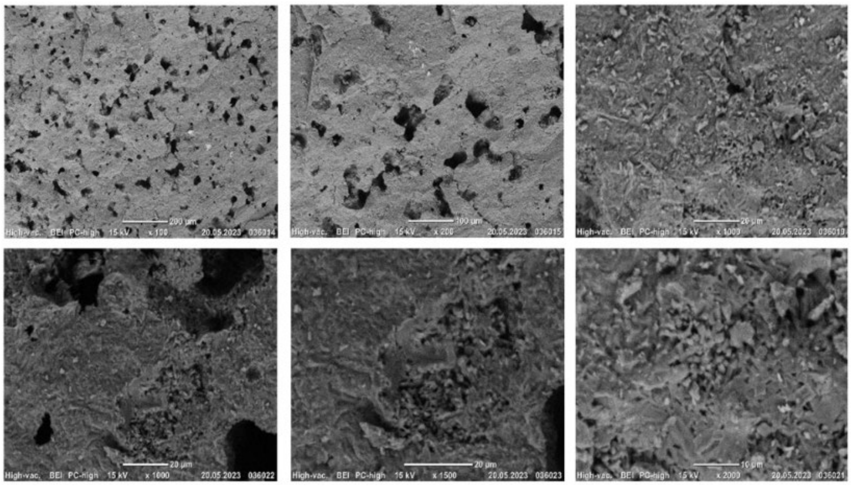

Figure 12. Electron micrographs of cleavage of semi-dry pressing samples from a mixture of refractory clay with the addition of 40 % steel slag ($C_{60}S_{40}$), fired at 1200 °C.

The introduction of a 40 % steel slag additive into the composition of the refractory clay used (composition $C_{60}S_{40}$) activates the process of liquid-phase sintering of the samples, which leads to the formation of a monolithic structure with separated internal pores, in shape approaching spherical, with a diameter of up to 20–25 microns (Fig. 12).

4. Conclusions

1. Steel slag in terms of chemical composition is represented mainly by oxides of calcium (35.33 %), iron (21.45 %), silicon (17.62 %), and aluminum (7.80 %), the sum of which is more than 80 %. In terms of mineralogical composition, it is composed of portlandite $Ca(OH)_2$, silicates, and hydrated silicates of calcium and magnesium (enstatite $MgO•SiO_2$, okermanite $2CaO•MgO•2SiO_2$, tobermorite $5CaO•6SiO_2•5H_2O$ and dicalcium hydrosilicate $2CaO•SiO_2•H_2O$), aluminates and calcium ferrites (monocalcium aluminate $CaO•Al_2O_3$, monocalcium ferrite $CaO•Fe_2O_3$).
2. The crystalline component of steel slag after heating in the temperature range of 1100–1300 °C is represented by a mixture of okermanite $2CaO•MgO•2SiO_2$, monocalcium aluminate $CaO•Al_2O_3$, enstatite $MgO•SiO_2$, and dicalcium silicate γ–$2CaO•SiO_2$ polymorphism, which causes complete destruction of the molded samples after cooling.

3. The use of steel slag to produce ceramic materials is possible only by neutralizing the destructive effect of dicalcium silicate formed in steel slag at firing temperatures above 1000 °C, converting it into other calcium-containing minerals without destroying molded products.
4. Compositions of refractory clay with additions of steel slag from 30 to 40 % at a firing temperature of 1175–1200 °C form ceramic structures with water absorption from 2.8 to 13.4 %, with a compressive strength of 1.7–2.8 times the strength samples from the studied clay without additives (97–215 MPa and 56 MPa, respectively), which determines their prospects for producing high-strength anorthite ceramics for a wide range of purposes.

References

1. Ezerskiy, B.A. Clinker. Technology and properties. Stroitel'nye Materialy [Construction Materials]. 2011. Pp. 79–81.
2. Ezerskiy, V.A. Quantitative assessment of the color of ceramic face products. Stroitel'nye materialy [Construction Materials]. 2015. 8. Pp. 76–80. DOI: 10.31659/0585-430X-2015-728-8-76-80
3. Crespo-López, L., Cultrone, G. Improvement in the petrophysical properties of solid bricks by adding household glass waste. Journal of Building Engineering. 2022. 8. Article no. 105039. DOI: 10.1016/j.jobe.2022.105039
4. Vakalova, T.V., Revva, I.B. Highly porous building ceramics based on «clay-ash microspheres» and «zeolite-ash microspheres» mixtures. Construction and Building Materials. 2022. 317. Article no. 125922. DOI: 10.1016/j.conbuildmat.2021.125922
5. Shi, C. Steel slag – its production, processing, characteristics, and cementitious properties. Journal of Materials in Civil Engineering. 2004. 16(3). 230–236. DOI: 10.1061/(ASCE)0899-1561(2004)16:3(230)
6. Sun, P., Guo, Z. Preparation of steel slag porous sound-absorbing material using coal powder as pore former. Journal of Environmental Sciences. 2015. 36. Pp. 67–75. DOI: 10.1016/j.jes.2015.04.010
7. Wang Q., Yan, P., Feng, J. A discussion on improving hydration activity of steel slag by altering its mineral compositions. Journal of Hazardous Materials. 2011. 186(2–3). Pp. 1070–1075. DOI: 10.1016/j.jhazmat.2010.11.109
8. Shi, C., Qian, J. High performance cementing materials from industrial stags – a review. Re-sources, Conservation and Recycling. 2000. 29(3). Pp. 195–207. DOI: 10.1016/S0921-3449(99)00060-9
9. Tüfekçi, M., Demirbaş, E.A., Genç, H. Evaluation of steel furnace slags as cement additives. Cement and Concrete Research. 1997. 27(11). Pp. 1713–1717. DOI: 10.1016/S0008-8846(97)00158-0
10. Kourounis, S., Tsivilis, S., Tsakiridis, P.E., Papadimitriou, G.D., Tsibouki, Z. Properties and hydration of blended cements with steelmaking slag. Cement and Concrete Research. 2007. 37(6). Pp. 815–822. DOI: 10.1016/j.cemconres.2007.03.008
11. Beshr, H., Almusallam, A.A., Maslehuddin, M. Effect of coarse aggregate quality on the mechanical properties of high strength concrete. Construction and Building Materials. 2003. 17(2). Pp. 97–102. DOI: 10.1016/S0950-0618(02)00097-1
12. Wu, Z., Feng, Z., Pu, S., Zeng, C., Zhao, Y., Chen, C., Song. H., Feng, X. Mechanical properties and environmental characteristics of the synergistic preparation of cementitious materials using electrolytic manganese residue, steel slag, and blast furnace slag. Construction and Building Materials. 2024. 411. Article no. 134480 DOI: 10.1016/j.conbuildmat.2023.134480
13. Gu, X., Wang, H., Liu, J., Zhu, Z., Wang, S., Xu, X. Synergistic effects of steel slag and metakaolin in cementitious systems: Packing properties, strength, and microstructure. Construction and Building Materials. 2024. 411. Article no. 134395. DOI: 10.1016/j.conbuildmat.2023.134395
14. Chen, G., Wang, S. Research on macro-microscopic mechanical evolution mechanism of cement-stabilized steel slag. Journal of Building Engineering. 2023. 75. Article no. 107047. DOI: 10.1016/j.jobe.2023.107047
15. Aliyah, F., Kambali, I., Setiawan, A.F., Radzi, Y.M., Rahman, A.A. Utilization of steel slag from industrial waste for ionizing radiation shielding concrete: A systematic review. Construction and Building Materials. 2023. 382. Article no. 131360. DOI: 10.1016/j.conbuildmat.2023.131360
16. Luo, T., Wang, X., Zhuang, S. Value-added utilization of steel slag as a hydration heat con-trolling material to prepare sustainable and green mass concrete. Case Studies in Construction Materials. 2023. 19. Article no. e02619. DOI: 10.1016/j.cscm.2023.e02619
17. Liu, L., Liu, J., Liu, T., Zhang, Y., Liang, H., Ning, T., Lin, X., Bai, Z., Lu, A. Preparation, crystallization kinetics and stabilization behavior of the heavy metal ions of all-solid waste-based glass-ceramics from steel slag and coal gangue. Journal of Non-Crystalline Solids. 2022. 592. Article no. 121750. DOI: 10.1016/j.jnoncrysol.2022.121750
18. Deng, L., Yun, F., Jia, R., Li, H., Jia, X., Shi, Y., Zhang, X. Effect of SiO_2/MgO ratio on the crystallization behavior, structure, and properties of wollastonite-augite glass-ceramics derived from stain-less steel slag. Materials Chemistry and Physics. 2020. 239. Article no. 122039. DOI: 10.1016/j.matchemphys.2019.122039
19. Luo, Z., He, F., Zhang, W., Xiao, Y., Xie, J., Sun, R., Xie, M. Effects of fluoride content on structure and properties of steel slag glass-ceramics. Materials Chemistry and Physics. 2020. 242. Article no. 122531. DOI: 10.1016/j.matchemphys.2019.122531
20. 20. Pioro, L.S., Pioro, I.L. Reprocessing of metallurgical slag into materials for the building industry. Waste Management. 2004. 24(4). Pp.371–379. DOI: 10.1016/S0956-053X(03)00071-0
21. Zong, Y., Chen, W., Fan, Y., Yang, T., Liu, Z., Cang, D. Complementation in the composition of steel slag and red mud for preparation of novel ceramics. International Journal of Minerals, Metallurgy and Materials. 2018. 25(9). Pp. 1010–1017. DOI: 10.1007/s12613-018-1651-2
22. Bantsis, G., Sikalidis, C., Betsiou, M., Yioultsis, T., Bourliva, A. Ceramic building materials for electromagnetic interference shielding using metallurgical slags. Advances in Applied Ceramics. 2011. 110(4). Pp. 233–237. DOI: 10.1179/1743676111Y.0000000009
23. El-Mahllawy, M.S. Characteristics of acid resisting bricks made from quarry residues and waste steel slag. Construction and Building Materials. 2008. 22(8). Pp. 1887–1896. DOI: 10.1016/j.conbuildmat.2007.04.007
24. Rahou, H., Rezqi, M., Ouahabi, N., Fagel. Characterization of Moroccan steel slag waste: The potential green resource for ceramic production. Construction and Building Materials. 2022. 314(B). Article no. 125663. DOI: 10.1016/j.conbuildmat.2021.125663

25. Karayannis, V.G., Moutsatsou, A.K., Baklavaridis, A.N., Katsika, E.L., Domopoulou, A.E. Synergistic Sintering of Lignite Fly Ash and Steelmaking Residues towards Sustainable Compacted Ceramics. Advances in Materials Science and Engineering. 2017. Article no. 1735268. DOI: 10.1155/2017/1735268
26. Teo, P.T., Anasyida, A.S., Kho, C.M., Nurulakmal, M.S. Recycling of Malaysia's EAF steel slag waste as novel fluxing agent in green ceramic tile production: Sintering mechanism and leaching assessment. Journal of Cleaner Production. 2019. 241. Article no. 118144 DOI: 10.1016/j.jclepro.2019.118144
27. Cao, P., Xing, L., Luo, J., Jiang, H., Zhang, X., Li, G. Preparation of calcium silicate board from to-bermorite-rich residue for energy conservation in buildings. Construction and Building Materials. 2023. 407. Article no. 133547. DOI: 10.1016/j.conbuildmat.2023.133547
28. Wesselsky, A., Jensen, O.M. Synthesis of pure Portland cement phases Cement and Concrete Re-search. 2009. 39(11). Pp. 973–980. DOI: 10.1016/j.cemconres.2009.07.013
29. Vakalova, T.V., Sergeev, N.P., Tolegenov, D.T., Tolegenova, D.Zh. High-strength building ceramics based on fly ash – red mud mixtures. Magazine of Civil Engineering. 2023. 121(5). Article no. 12104. DOI: 10.34910/MCE.121.4
30. Shakhov, S.A. Structural and phase features of ceramics from loam and incinerated sewage sludge ash. Magazine of Civil Engineering. 2023. 121(5). Article no. 12110. DOI: 10.34910/MCE.121.10

Information about the authors:

Tatiana Vakalova, *Doctor of Technical Sciences*
ORCID: https://orcid.org/0000-0002-1756-3526
E-mail: tvv@tpu.ru

Nikolay Sergeev,
ORCID: https://orcid.org/0000-0002-7656-5628
E-mail: axioma-13@yandex.ru

Dias Tolegenov,
ORCID: https://orcid.org/0000-0001-8242-0655
E-mail: www.dika-92@mail.ru

Inna Revva, *PhD in Technical Sciences*
ORCID: https://orcid.org/0000-0003-4184-1554
E-mail: revva@tpu.ru

Received 17.02.2024. Approved after reviewing 06.09.2025. Accepted 07.09.2025.